Atmos. Chem. Phys. Discuss., 10, 3053–3086, 2010
www.atmos-chem-phys-discuss.net/10/3053/2010/

Atmospheric Chemistry and Physics Discussions

Impacts of dust on West African climate during 2005 and 2006

M. Camara[1,4], G. Jenkins[2], and A. Konare[3]

[1]Département de Physique, Université de Ziguinchor, BP 523, Ziguinchor, Senegal
[2]Physics and astronomy department, Howard University, DC, 20059, USA
[3]Université de Cocody, Abidjan 22, BP 582, Côte d'Ivoire
[4]Laboratoire de Physique de l'atmosphère – SF, BP 5085 Dakar-Fann, Senegal

Received: 30 August 2009 – Accepted: 7 January 2010 – Published: 5 February 2010

Correspondence to: M. Camara (moctar1sn@yahoo.fr)

Published by Copernicus Publications on behalf of the European Geosciences Union.

Abstract

The aim of this study is to understand the impacts of Saharan dust outbreaks on West African climate using a 3-dimensional, hydrostatic, sigma vertical coordinate regional climate model (RegCM). We performed a simulation with the non aerosol version of the model (control case) followed by another simulation using the desert dust module (dust case) implemented in RegCM which includes emission, transport, gravitational settling, wet and dry removal and calculation of dust optical properties for 2005 and 2006. Dynamic and thermodynamic parameters obtained from both versions of the model are intercompared and validated with NCEP/NCAR reanalysis, African Monsoon Multidisciplinary Analysis (AMMA) program data and the Global Precipitation Climatology Project (GPCP) rainfall products. The spatial and temporal distribution of the Aerosol optical depth derived from the desert dust run is compared to available observed aerosol data such as the Aerosol Robotic Network (AERONET) program and satellites data.

Using radiosounding data and RegCM outputs, a case study of a strong dust outbreak showed the presence of a stable environment at Dakar, Sal and Nouadhibou stations.

1 Introduction

The indirect and direct aerosol effects play an important role for climate (Penner et al., 2001; Cubasch et al., 2001). Aerosols are produced through natural processes (desert dust lifting, sea spray, volcanic eruption, etc.) and anthropogenic activities, such as biomass burning. Saharan desert dust which is produced through suspension, saltation and creeping processes associated with wind erosion is the main aerosol component in Sahel-Saharan region during the boreal summer.

Sahara desert is the world's largest source region of dust (Goudie and Middleton, 2001). An estimated 1600×10^6 tons of dust particles is lifted annually from the Sahara desert and transported westward by easterly winds (Ozer, 2001). Dust can travel long

ACPD

10, 3053–3086, 2010

Impacts of dust on West African climate during 2005 and 2006

M. Camara et al.

distances in the atmosphere and can be detected as far as Florida and American coast (Shiin et al., 2000; Walsh and Steidinger, 2001). An elevated layer of dry air and mineral dust between 500–850 hPa called Saharan Air Layer (SAL) may impact Atlantic tropical cyclones between 10° N and 20° N by inhibiting their ability to intensify (Dunion and Velden, 2004). Evan et al. (2006) found significant positive correlation between dust cover and Atlantic tropical cyclone days. Using satellite derived index, Engelstaedter and Washington (2007) showed that the annual dust cycle in West Africa is related to small-scale high-wind event.

Although dust radiative processes are likely more important at regional scale, fewer studies have been dedicated to the inclusion of dust processes on regional climate models (Gong et al., 2003; Song and Carmichael, 2001) and especially over West Africa.

Zakey et al. (2006) implemented a dust module in a regional climate model (RegCM) to study the Saharan dust distribution and compared their simulations outputs to available observed aerosols data such as TOMS index and Aeronet program aerosol optical depth. They conducted two Saharan dust events simulation and also a 3 month (June-July-August 2000) simulation over a region that encompassed West Africa and Europe. They found that the model reproduces the main spatial and temporal features of the dust distribution especially at seasonal timescale over the Saharan region. They concluded that the coupled model is suitable for long-term simulation of dust effects on West African and European climate.

Konare et al. (2008) used the same model (RegCM3) to simulate 38 West African summer seasons (June-July-August-September) from 1969 to 2006 and intercompared runs with and without dust radiative effects. They found that the radiative shortwave forcing of dust is to reduce the precipitation over the Sahel, to strengthen the southern branch of the AEJ and to weaken the Tropical Eastery Jet. Konare et al. (2007) did not take into account the longwave radiative forcing of dust. Solmon et al. (2008) investigated the shortwave and the longwave radiative forcing of Saharan dust on West African monsoon system and found similar results with Konare et al. (2008).

Modeling studies with general circulation models have been extensively conducted to characterize dust effects on climate. Yoshioka et al. (2007) used a general circulation model in which a dust module was implemented to study the effects of dust on Sahel rainfall. Their simulations were either forced by the observed sea surface temperature (SST) or coupled with the interactive SST using an ocean model. When they activated the dust radiative forcing, they found a rainfall decrease in the Inter tropical Convergence Zone (ITCZ) including Sahel region coupled with an increase south of the ITCZ in the interactive SST simulations. The rainfall distribution is affected only over the North Africa in their SST-forced simulations. Miller and Tegan (1998) found a surface temperature reduction of 1 K under the dust layer in regions where deep convection is absent. These authors also suggest that the presence of dust in the atmosphere results in a surface cooling and a warming of the dust-laden air which could suppress cloud formation. This result is consistent with Lau and Kim (2007) studies who found that increased (decreased) Saharan dust is associated with cooling (warming) of the Atlantic Ocean during the hurricane season due to reduced incoming solar radiation during dust episodes.

Despite these important studies, the temporal and spatial distributions of dust as well as its impacts on climate are still not well understood.

This study aims to understand the temporal, horizontal and vertical distributions of Saharan dust and to characterize its effects on West African climate at daily, seasonal and annual timescale using a regional climate model (RegCM3) and available observed data for the period of 2005 and 2006.

2 Model description and experiment

RegCM is a hydrostatic regional model developed at the Abdu Salam International Centre for Theoretical Physics (ICTP) (Giorgi et al., 1993a,b) whose radiative processes are from the NCAR global model CM3 (Keihl et al., 1996). The dynamics of the model is mostly the same as the hydrostatic version of MM5 (Grell et al., 1994). Grell scheme

ACPD
10, 3053–3086, 2010

has been used in our simulation to describe moist convection; this parameterization represents well rainfall distribution over West Africa (Jenkins et al., 2005). Biosphere Atmosphere Transfer Scheme (BATS, Dickinson et al., 1993) is used to describe land surface processes and this interface offers most of the parameters used to couple the dust emission.

The dust module of RegCM is extensively described in Zakey et al. (2006) and a brief description is given in Konare et al. (2008). The dust scheme of RegCM includes dust transport by wind, deep convection, turbulent diffusion and removal wet and dry processes and gravitational settling. The emission process is controlled by wind intensity and surface characteristics. A model grid point is considered to be either totally covered or not with desert dust. In our simulations, the lateral boundary and initial conditions used to drive the model are from the 6-h interval NCEP/NCAR reanalyses. The grid spacing and the top of the model are, respectively 60 km and 50 hPa. The model has been integrated from 1 November 2004 to 31 December 2006 using or not the dust module to study the daily, seasonal and annual spatial distribution of Saharan dust and the effects of its shortwave radiative forcing on West African climate especially on the Sahel-Saharan zone (region lies between 10° N and 30° N) during 2005 and 2006.

We conducted two simulations which include dust parameterization (dust case) or not (control case) and intercompared results. The model outputs have been also validated with available observed data. This study is divided into three parts:

The first part of this paper focuses on dust spatial (both horizontal and vertical) and temporal characteristics. We compare the aerosol optical depth derived from the dust module simulation to the observed Aerosol Robotic Network (AERONET) data (http://aeronet.gsfc.nasa.gov/) and the Total Ozone Mapping Spectrometer (TOMS) aerosol index (http://toms.gsfc.nasa.gov/).

The second part of the paper focuses on the comparison of the annual and seasonal cycles of atmospheric parameters derived from the control and the dust runs to characterize dust effects on West African climate. Models dynamic and thermodynamic outputs are compared to the NCEP/NCAR reanalysis data described in Kalnay

ACPD
10, 3053–3086, 2010

et al. (1996) and the GPCP rainfall products (http://precip.gsfc.nasa.gov).

Finally, a case of a strong dust outbreak (10 September 2006) is studied using the dust version outputs, satellite products and African Monsoon Multidisciplinary Analysis radiosounding data.

3 Results

3.1 Dust characteristics

The TOMS aerosol index (AI) is used to compare satellite observations to the RegCM's horizontal distribution of dust during the summer period. This index has been widely used by the scientific community to validate aerosol optical depth derived from desert dust models. The TOMS AI is used to detect dust in the near UV (Herman et al., 1997; Torres et al., 1998) by measuring the change of spectral contrast due to radiative transfer effects of aerosols in a Raleigh scattering atmosphere. TOMS AI can be considered at a first approximation as proportional to the aerosol optical depth. Figure 1 shows TOMS AI in July, August, and September (JAS) averaged over 2005 and 2006. Dust is mainly located northward of 10° N in July-August-September period. In July, 3 maxima appear. The first maximum extends from Mauritania-Morocco border to Mauritania-Algeria border and the second and the third maxima are located, respectively between 8° W–2.5° E and around 17.5° E. During August, the second maximum is still well defined while the first and the third maxima are weak. In September, only the eastern maximum is present.

The horizontal distribution of the aerosol optical depth (AOD) and the vertical profile of the aerosol extinction coefficient derived from the dust version of RegCM for July, August and September averaged over 2005 and 2006 are shown in Fig. 2. During the boreal summer, dust is present mainly northward of 10° N with 2 maxima. The first and larger maximum is located over Mauritania-Mali border (around 17.5° N–22° N; 15° W–0° W). This maximum decreases from July to September and is located further west

ACPD
10, 3053–3086, 2010

(18° N, 10° W) in September. We have a second maximum around 17° N and 12.5° E over Niger which also decreases from July to September. During September a third maximum weaker than the 2 others is located around 27.5° N, 0° W over Algeria. The July–August maxima are shifted westward when compared to TOMS aerosol index.

The vertical profile of the aerosol extinction coefficient performed over the area of the maximum aerosol optical depth (between 10° W and 0° W) shows that dust extends from the surface to 500 hPa and its maximum is located near the surface (between 1000 hPa and 850 hPa) at around 20° N for July, August and September. As for the horizontal distribution of AOD, we noticed a weakening in the vertical profile of the aerosol extinction coefficient from July to September. The vertical profile of dust concentration presents the same patterns than the aerosol extinction coefficient (figure not shown).

To study the temporal distribution of dust, we represent in Fig. 3 the seasonal cycle of the vertical profile of the aerosol extinction coefficient for 2 Western Sahel stations which are Sal (Cabo Verde, 16.43° W–22.56° N) and Dakar (Senegal, 16.57° W–14.23° N) and 2 Eastern Sahel stations: Agoufu (Mali 1.28° W–15.2° N) and Banizoumbou (Niger, 2.5° E–13.3° N). Except for Sal station, the aerosol extinction coefficient shows two maxima around March and June–July. The maximum occurring in March is located at low to mid-levels while during June–July strong values are mainly concentrated at mid-levels. The June–July maximum is stronger and broader than the March one, except for Banizoumbou station. During the month of March, Dakar station shows the greatest values of dust content. While in June–July, Sal station presents the strongest aerosol extinction coefficient values. Banizoumbou station is less affected by dust than the other stations throughout the year in agreement with Engelstaedter and Washington (2007).

We compare the annual cycle of aerosol optical depth simulated by the model to AERONET data in Fig. 4. At Sal station, RegCM and AERONET aerosol optical depth present similar values and trends from January to June followed by a slight overestimation by the model from July to September. There's no available AERONET data from October to December. Dakar station shows an anticorrelation between AERONET and

RegCM simulation from March to April with an overestimation by the model. A similar trend of AOD with a slight overestimation by the model is depicted from June to September followed by similar values and trend from October to December.

The eastern stations Banizoumbou and Agoufu show the same characteristics with an underestimation of the AOD by the model. This underestimation by the model is larger from January to June (respectively from March to July) for Banizoumbou (respectively Agoufou). This may be due to an underestimation of dust outbreaks from the Bodele Depression located around 16° E, 17° N.

We represent in Fig. 5 the daily mean of the model and the Aeronet aerosol optical depth for the boreal summer of 2006 (July through September) for the same 4 stations during the AMMA SOP period.

For Sal (Cabo Verde) station, the model values are generally stronger than the Aeronet data. However, data interpretation is limited by lot of missing Aeronet data (two third) at SAL. The coefficient of correlation between RegCM and AERONET data is weak (24%).

The model strongly underestimates (overestimates) two events during the 2nd half of July (respectively during August) at Dakar (Senegal) station. The mean AOD is 0.52 for the model and 0.43 for the Aeronet in the July–September period. The number of days where the AOD is stronger than 0.43 is 43 for RegCM and 32 for Aeronet suggesting that RegCM simulates more strong dusty days than the observed data. The coefficient of correlation for Dakar is slightly stronger than SAL station (26%).

Agoufou station shows a better correlation between observed and model data (60%). The mean AOD is 0.52 for RegCM and 0.50 for Aeronet. The number of days with AOD greater than 0.5 is the same (41 days) for the two datasets.

For Banizoumbou station, the model fails to simulate two strong dust events around 10 August and 8 September. The mean AOD is 0.36 for RegCM and 0.34 for Aeronet. The number of days with AOD greater than 0.34 is 39 for RegCM and 34 for Aeronet suggesting that the number of strong dust events of the model is larger than the Aeronet data. The coefficient of correlation between observed and modeled data is weaker for

Banizoumbou (34%) than for Agoufou.

The influence of the horizontal and vertical dust distribution on meteorological parameters especially over the Sahel-Saharan region during the boreal summer is studied in the next section.

3.2 Effects of dust on environmental parameters during July-August-September (JAS)

The effects of dust on West African climate are studied by comparing the simulation which takes into account the Sahara desert dust (dust case) to the control case which had been performed without dust effects. Figure 6 shows the mean July–September 2005–2006 of surface temperature, relative humidity at mid-levels (700 hPa) and solar radiation absorbed at the surface for the control case (left) and the difference between dust and control cases (right).

During the boreal summer, a northward increase of surface temperature is noticed in the control run with a maximum over the Saharan region. Mid-levels humidity is strong over the Eastern part of West Africa. As for surface temperature, solar radiation absorbed at the surface increases from south to north over West Africa.

The largest changes in temperature and relative humidity are generally found northward of 10° N when dust effect is taken into account. The inclusion of dust result in a reduced incoming solar radiation (absorption and reflection of sunlight by dust particles) and then a surface cooling especially in regions where the AOD is maximum (Fig. 6; top). When considering the specific humidity, a strong dry layer is present northward of 15° N and between 10° W–10° E at mid-levels when dust parameterization is taken into account (Fig. 6; middle).

Figure 6 (bottom; right) shows strong negative values under the maximum dust coverage (particularly around 2.5° W, 20° N) implying that dust strongly decreases the amount of solar radiation absorbed at the surface (reduced by as much as 80 W m^{-2} at some locations) and hence surface temperatures.

In order to go further in the characterization of dust effects on temperature and humidity, the vertical profile of the difference between the dust and control case for the temperature and the specific humidity averaged over July–September 2005–2006 is displayed in Fig. 7. Figure 7 shows a surface cooling and a dry environment at mid-levels as previously diagnosed in Fig. 6. Over the Northern Sahel and Saharan region (17.5° N–27.5° N), the cooling extends up to 600 hPa and there's a warming above suggesting that solar radiation is partially absorbed in the first meters of dust layers resulting in a warming in those areas and a cooling below. The cooling is stronger especially near the surface (−1.6 °C) than the above warming. The low-levels cooling is stronger in July followed by September during the summer period (figure not shown). The specific humidity increases slightly at low-levels and decreases strongly at the mid-levels (−0.001 kg/kg) when dust parameterization is included.

The dynamic conditions are investigated using the boreal summer (Mean July–September 2005–2006) wind distributions at low (925 hPa), middle (700 hPa) and upper (200 hPa) levels. Wind conditions for the NCEP/NCAR reanalysis are represented in Fig. 8.

Wind at 925 hPa is used to study the monsoon flow which advects sufficient moisture from the ocean to the continent to allow deep convection to take place in the Sahelo-Saharan region during the boreal summer. The monsoon flow extends up to 18° N over West Africa and is stronger (6 m/s) between 5° N and 10° N when considering the reanalysis data. At 700 hPa, the main features of West African climate are the African Easterly jet and the African easterly waves. The AEJ results from the temperature contrast between the cool low-levels wind flow from the Guinea Gulf and the hot Saharan desert air (Burpee, 1972) and it extends from Lake Chad to Capo Verde.

The mixed baroclinic and barotropic conversion in the AEJ is the source of the African easterly waves (Burpee). These waves propagate westward with a period of 3–5 days and modulate daily rainfall over the West Africa and initiate most tropical cyclones over the North Atlantic (Carlson et al., 1969; Burpee, 1972; Reed et al., 1977). The AEJ core extends from Eastern Africa to 50° W over the ocean with a maximum of 10 m/s (Fig. 8; middle). At upper levels, the Tropical easterly jet originates from the contrast temperature between the Tibetan region and oceanic region near the equator. The TEJ may be strengthened by latent heat released over Africa by deep convection (Janicot, 1990). The TEJ is mainly located between 0° N and 10° N with a maximum of 16 m/s around 15° W and 3° N (Fig. 8; bottom).

Wind conditions during the boreal summer for RegCM model are represented in Fig. 9.

The low-levels monsoon flow doesn't show any systematic difference between the control and the dust case. But the monsoon air is stronger over the northern part of Sahel (15° N–20° N) for the control case. This result is consistent with the existence of a deeper Saharan heat low around 20° N–25° N (figure not shown) which may favors the deeper penetration of the humid monsoon air over West Africa for the control run. This lesser penetration of the monsoon flow in the dust case is also consistent with the surface cooling which results in the decrease of the meridional gradient of moist static energy and then the monsoon flow (Konare et al., 2008; Solmon et al., 2008).

AEJ is stronger south of 14° N over Western Sahel (10° W–0° W) and off West African coast in the dust case. TEJ is stronger west of 7.5° W for the control run than for the dust case. Some authors (Grist and Nicholson, 2001; Janicot, 1992) found that a dry Sahel year is characterized by a weak monsoon flow over the Sahel, a strong and southward shift of AEJ and a weak TEJ suggesting that the inclusion of dust in the model may result in reducing precipitation over the Sahel region.

When comparing these two runs to the NCEP/NCAR reanalysis data, we noticed that the two versions of the model capture well the structure of the monsoon flow, African easterly jet and the tropical easterly jet. However all versions show weaker monsoon flow over the Sudan-Guinean region (6 m/s for NCEP/NCAR reanalyses versus 4 m/s for the model runs). The dust version shows similar northward propagation of the monsoon flow with the NCEP reanalysis. At the mid-levels, the African easterly jet strength is slightly stronger (2 m/s difference) for the two RegCM runs than for the NCEP reanalysis. At upper levels, the tropical easterly jet is also stronger for the model with a difference of 6 m/s over some regions.

ACPD
10, 3053–3086, 2010

To study the degree of atmospheric instability, we represent in Fig. 10 the vertical velocity (Pa/s) for the two cases. Two ascending regions are shown with the first region which extends up to 200 hPa, is located between 5° N–12.5° and is linked to the deep convection associated with the Inter Tropical convection zone (ITCZ). The second zone of upward winds is located around 22° N and is limited to 600 hPa. This ascending zone is the result of the convergence of the humid and cooler low levels south-westerly wind and the dry and hot northerly air from the Saharan Desert. The ascending zones are stronger for the control run suggesting that the atmosphere is more unstable in that case than for the dust run. The vertical velocity values for the northern ascending region are stronger for both versions of the model (bias of 0.02 Pa/s to 0.04 Pa/s) compared to the NCEP/NCAR reanalysis data. Deep convection in the Southern region is stronger at low levels for the reanalysis. The model runs show stronger convection at mid-levels and weaker convection at the upper levels when compared to the reanalysis data.

The annual cycle of West African rainfall is represented in Fig. 11. The model results are validated with Global Precipitation Climate Project (GPCP) rainfall products which consist of monthly means of precipitation derived from satellites and gauge measurements.

This figure shows that the maximum of rainfall moves rapidly from 5° N (Guinea region) from June to 10° N around July-August-September period for the GPCP rainfall. This rapid and discontinuous northward shift of the maximum rainfall from the Guinea region to the Sahel zone during the boreal is known as the West African monsoon jump (Sultan and Janicot 2003). The Guinea maximum is underestimated (3 mm/day) by both versions of the model.

Over the Sahel region (10° N–20° N) and during the peak of Sahel rainfall (July through September), precipitation is stronger and extends further north for the control run than for the dust case suggesting that the implementation of the dust module in RegCM results in a decrease of rainfall over the Sahel in coherence with GPCP precipitation. This result suggests that the dust implementation in the model improve the

ACPD
10, 3053–3086, 2010

summer rainfall strength over the Sahelian region. Weaker values of potential of instability are noticed in the Sahel region in the dust case (figure not shown) suggesting that the presence of a more stable environment which is not favorable for strong convection and rainfall. This reduction of precipitation over the Sahel is also consistent with the monsoon flow, AEJ and TEJ patterns found in Fig. 9 and also with Konare et al. (2008) studies. These results also are consistent with Miller and Tegen (2004) and Yoshioka et al. (2007) who found a decrease of Sahel rainfall when implementing a dust module in a general circulation model.

3.3 A case study of a strong dust outbreak

We represent in Fig. 12 the case of a strong dust outbreak (10 September 2006) which affects several countries such as Senegal, Mauritania and Capo Verde. This outbreak is captured as well as by the TOMS aerosol product and by the RegCM model. These data show that strong dust values are present over Mauritania and Capo Verde. Table 1 summarized aerosol optical depth values calculated with RegCM for the stations of Nouadhibou (Mauritania), Sal (Capo Verde) and Dakar (Senegal) at 00:00 UTC and 12:00 UTC. AOD is stronger at nighttime (00:00 UTC) for all stations especially for Nouadhibou (1.86). Dust effects on dynamic and thermodynamic profiles are studied by comparing the temperature, dewpoint temperature, zonal and meridional wind profiles derived from RegCM to the radiosounding data of the AMMA program.

We also used two instability indexes in order to go further in the characterization of the degree of instability during dust outbreaks: the Convective Available Potential Energy (CAPE) and the Convective Inhibition (CIN). The CIN is the energy needed to lift an air parcel vertically and pseudo adiabatically from its originating level to its level of free convection (LFC).

$$\mathrm{CIN} = \int_{P_s}^{\mathrm{LFC}} (T_{\mathrm{va}} - T_{\mathrm{v}}) R_{\mathrm{a}} d(\ln(P)) \tag{1}$$

ACPD
10, 3053–3086, 2010

Impacts of dust on West African climate during 2005 and 2006

M. Camara et al.

CAPE is the maximum energy available to ascending a parcel from its level of free convection to its equilibrium level.

$$\mathrm{CAPE} = -\int_{\mathrm{LFC}}^{\mathrm{EL}} (T_{\mathrm{va}} - T_{\mathrm{v}}) R_{\mathrm{a}} d(\ln(P)) \tag{2}$$

LFC is the level of free convection;
EL is the equilibrium level;
R_a is the constant of ideal gaz;
T_v is the virtual temperature of the parcel;
T_{va} is the virtual temperature of environmental air;
P is the pressure;
P_s is the surface pressure;

Higher (lower) values of CAPE (CIN) indicate greater potential for severe weather. Both CAPE and CIN are among the best indexes for determining the instability of atmospheric layers.

We compute these parameters at 00:00 UTC for Dakar and Sal and at 12:00 UTC for Nouadhibou station because of the lack of radiosounding data at 00:00 UTC for that station. Results are presented in a Skew-T plot with the dust model at the right and the radiosounding data at the left (Fig. 13). The black (green) profile represents the sounding temperature Tsnd (dewpoint temperature Dsnd). Wind barbs are displayed at the right of the plot. At the right corner, some thermodynamic parameters such as the CAPE and the CIN are displayed.

When considering Dakar and Sal stations, an inversion layer is found around 900 hPa followed by a dryness (strong values of Tsnd-Dsnd) of the layer from 900 hPa to 300 hPa for both datasets. Winds are mainly easterly for Dakar throughout the troposphere except for low-levels where they are South-Easterly for the radiosounding data and North-Westerly for the model. At Sal station, winds blow from West at low-levels and East between 950 hPa and 50 hPa for the model. For the radiosounding data, winds are South-Easterly from the surface to 500 hPa, Northerly from 500 hPa to 150 hPa and Easterly above that layer.

CAPE and CIN values derived from the model are weak for Dakar suggesting that the environment is stable. For Sal, the CAPE is also weak but there's a strong CIN suggesting the existence of a strong stable environment. CAPE (CIN) remains high (low) at Sal and Dakar stations for the radiosounding data.

Two inversions zones exist for Nouadhibou at 900 hPa and at 600 hPa in the RegCM output. Nouadhibou station is affected by South-Easterly wind at the low levels and an easterly wind at mid to upper levels. This station exhibits the strongest CIN (408 j/kg) accompanied by a weak CAPE suggesting the presence of a stable environment. A strong value of CAPE is noted; the convective inhibition does not exist.

Nouadhibou station is affected by south to south-easterly winds at low-levels for the model output. The magnitude of the wind is stronger for the model than for the radiosounding data. The difference between the temperature and dewpoint temperature (Tsnd-Dsnd) remains high throughout the troposphere for the radiosounding data suggesting the presence of a stable environment in coherence with the model output. CAPE and CIN are equal to zero for the radiosounding data.

4 Summary and conclusion

The aim of this study was to characterize the daily, seasonal and annual cycle of dust distribution over West Africa and its effects on West African climate during the boreal summer using a regional climate model. Dust characteristics, dynamic and thermodynamic conditions derived from the two sets of runs (with and without dust shortwave radiative feedbacks) have been compared to satellite, radiosounding and NCEP reanalysis data. The main results can be summarized as follows.

The model aerosol optical depth is located mainly northward of 10° N and presents 3 maxima located over Mauritania-Mali border, Niger and Algeria (during September). The first two maxima are stronger during July–August than September. While the

Algeria maximum exist only in September. The dust layer extends from the surface to 500 hPa with a maximum near the surface for July, August and September. Satellites data (TOMS aerosol index) show that dust is located mainly northward of 10° N as for the RegCM model. But the model July–August maxima are shifted westward when compared to TOMS aerosol index.

The aerosol optical depth derived from the model at 4 West African stations shows some similarities with the one measured with the AERONET program but there are some discrepancies. These differences from the observations data may be partially linked to the underestimation of Bodele Depression (Chad) and the dust parameterization in the model which does not take into account the effects of the sub-grid fractional dust emission; a grid cell is considered totally covered or not by desert dust.

From the point of the view of the thermodynamic, the effect of dust is to strongly reduce the temperature especially near the surface and humidity at the mid-levels. Vertically, temperature increase in the first layers of dust layer and decrease strongly near the surface. The relative humidity exhibits opposite characteristics especially at mid levels.

Wind derived from the model presents similar characteristics than the NCEP reanalysis data. However AEJ and TEJ are larger in both versions than in the NCEP reanalysis. On the other hand the monsoon flow is weaker in RegCM runs over the region lies between 5° N and 10° N. The monsoon flow strength over the northern part of Sahel which is strongly under dust influence is stronger for the control run than for the dust case in coherence with the existence of a deeper Saharan heat low which may favour the Northward and deeper penetration of the humid monsoon air. This result also is consistent with the surface cooling under the dust layer which results in a weakening of the moist static energy gradient and then the monsoon flow over the Northern Sahel. A strengthening (weakening) of the southern flank of AEJ (TEJ) is noticed in the dust case.

The vertical velocity maps show that the deep and the dry convection regions are stronger in the control run than for the dust case. Dry convection is stronger for the model runs than for the NCEP reanalysis. But deep convection exhibits opposite characteristics form low to high levels.

The seasonal cycle of rainfall is marked by a decrease of precipitation over the Sahel region when the dust scheme is introduced in coherence with the monsoon flow, AEJ and TEJ patterns. Precipitation over the Guinean region does not seem to be affected by dust inclusion in the model.

A case study of a strong dust outbreak over West African region on 10 September 2006 has been done in the last part of this study using the AMMA radiosounding data to characterize the impacts of dust on environmental conditions. A Very stable environment is present over Dakar, Sal and Nouadhibou when considering the model outputs and the radiosounding data.

In summary, RegCM3 model represents quite well the horizontal distribution of dust and the main features of West African climate such as the monsoon flux, the AEJ, TEJ and rainfall.

Dust impacts on Sahel-Saharan climate are mostly: strong cooling (warming) at the surface (mid-levels), a dry mid-levels environment, a less unstable environment, a weak monsoon flow over Northern Sahel, a southward strengthening of AEJ and a weak TEJ associated with a decrease of rainfall over Sahel. These results are consistent with those found with general circulation models simulations which showed a surface cooling under the dust layer (Miller and Tegen, 1998) and a decrease of rainfall over the Sahelian region during the boreal summer (Miller and Tegen, 2004; Yoshioka et al., 2007). Our results concerning the impacts of dust on West African climate during the summer season are also consistent with previous works performed with regional climate models (Konare et al., 2008; Solmon et al., 2008).

These results need to be confirmed by a study using a long temporal model run (1960 to 2006) in order to better understand the role of the African easterly jet and its associated African easterly waves in the reduction of Sahel rainfall when dust parameterization is introduced in the model. This long simulation can be used to characterize the dust strength and its distribution between the Sahel dry and wet years and therefore to address its role on the recent Sahel drought.

Acknowledgements. The authors are indebted to the International Centre for Theoretical Physics (ICTP) for the availability of the RegCM model, the Climate Diagnostics Center (NOAA, Boulder, CO, USA) for providing the NCEP/NCAR reanalysis database. Thanks to Brian Doty for the availability of the graphics software GrADS. This work was supported by Howard University (Washington DC, USA) and the University of Ziguinchor.

References

Berry, G. J. and Thorncroft, C. D.: Case study of an intense African easterly wave, Mon. Weather Rev., 133, 752–766, 2005.

Burpee, R. W.: The origin and structure of easterly waves in the lower troposphere of North Africa, J. Atmos Sci., 29, 77–90, 1972.

Carlson, T. N.: Some remarks on African disturbances and their progress, Mon. Weather Rev., 97, 716–728, 1969.

Dickinson, R., Henderson-Sellers, A., and Kennedy, P.: Biosphere-atmosphere transfer scheme (BATS) version 1e as coupled to the NCAR community climate model. Technical Report NCAR/TN-387+STR, NCAR Boulder, Colorado, 1993.

Dunion, J. P. and Velden, C. S.: The impact of the Saharan air layer on Atlantic tropical cyclone activity, B. Am. Meteorol. Soc., 85(3), 353–365, 2004.

Engelstaedter, S. and Washington, R.: Atmospheric control on the annual cycle of North African dust, J. Geophys. Res., 112, D03103, doi:10.1029/2006JD007195, 2007.

Giorgi, F., Marinucci, M., and Bates, G.: Development of a second generation regional climate model (RegCM). Part I: Boundary layer and radiative transfer processes, Mon. Weather Rev., 121, 2794–2813, 1993a.

Giorgi, F., Marinucci, M., and Bates, G.: Development of a second generation regional climate model (RegCM). Part II: Convective processes and assimilation of lateral boundary conditions, Mon. Weather Rev., 121, 2814–2832, 1993b.

Gong, S. L., Zhang, X. Y., Zhao, T. L., McKendry, I. G., Jaffe, D. A., and Lu, N. M.: Characterization of soil dust aerosol in China and its transport and distribution during 2001 ACE-Asia: model simulation and validation, J. Geophys. Res., 108(D9), 4262, doi:10.1029/2002JD002633, 2003.

Goudie, A. S. and Middleton, N. J.: Saharan dust storms: nature and consequences, Earth Sci.-Rev., 56(1–4), 179–204, 2001.
Grell, G. A.: Prognostic evaluation of assumptions used by cumulus parameterizations, Mon. Weather Rev., 121, 764–787, 1993.
Janicot, S.: Variabilité des précipitations en Afrique de l'Ouest et circulations quasi-stationnaires durant une phase de transition climatique, Thèse de doctorat, Paris VI, 600 pp., 1990.
Jenkins, G., Gaye, A., and Sylla, B.: Late 20th century attribution of drying trends in the Sahel from the Regional Climate Model (RegCM3), Geophys. Res. Lett., 32, L22705, doi:10.1029/2005GL024225, 2005.
Kalnay, E., Kanamitsu, M., Kistler, R., Collins, W. et al.: The NCEP/NCAR 40 year reanalysis project, B. Am. Meteorol. Soc., 77, 437–471, 1996.
Kiehl, J., Hack, J., Bonan, G. et al.: Description of the NCAR community climate model (ccm3), Technical report, National Center for Atmosheric Research, 1996.
Konare, A., Zakey, A. S., Solmon, F., Giorgi, F., Rauscher, S., Ibrah, S., and Bi, X.: A regional climate modelling study of the effects of desert dust on the West African monsoon, J. Geophys. Res., 113, D12206, doi:10.1029/2007JD009322, 2008.
Miller, R. L., Tegen, I., and Perlwitz, J.: Surface radiative forcing by soil dust aerosols and the hydrologic cycle, J. Geophys. Res., 109, D04203, doi:10.1029/2003JD004085, 2004.
Miller, R. L. and Tegen, I.: Climate response to soil dust aerosols, J. Climate, 11, 3247–3267, 1998.
Ozer, P.: Les lithometeores en region sahelienne, Int. J. Trop. Ecol. Geogr., 24, 1–317, 2001.
Penner, J. E., Andreae, M., Annegarn, H., Barrie, L., Feichter, J., Hegg, D., Jayaraman, A., Leaitch, R., Murphy, D., Nganga,J., Pitari, G., et al.: Aerosol, their direct and indirect effects, in: Climate Change 2001: the Scientific Basis, Contribution of Working Group I to the Third Assessment Report of the Intergovernmental Panel on Climate Change, edited by: Hougton, J. T., Ding, Y., Griggs, D. J. et al., Cambridge University Press, New York, chap. 5, 291–336, 2001.
Reed, R. J., Norquist, D., and Recker, E. E.: The structure and properties of African wave disturbances as observed during Phase III of GATE, Mon. Weather Rev., 105, 317–333, 1977.
Solmon, F., Mallet, M., Elguindi, N., Giorgi, F., Zakey, A., and Konare, A.: Dust aerosol impact on regional precipitation over Western Africa, mechanisms and sensitivity to absorption

properties, Geophys. Res. Lett., 35, L24705, doi:10.1029/2008GL035900, 2008.
Song, C. H. and Carmichael, G. R.: A three dimensional modelling investigation of the evolution processes of dust and sea-salt particles in East Asia, J. Geophys. Res., 103, 18131–18154, 2001.
Sultan, B. and Janicot, S.: The West African monsoon dynamics: Part II: The “preonset” and “onset” of the summer monsoon, J. Climate, 16, 3407–1586, 2003.
Walsh, J. J. and Steidinger, K. A.: Saharan dust and Florida red tides: the cyanophyte connection, J. Geophys. Res., 106(C6), 11597–11612, 2001.
Yoshioka M., Mahowald, N., Conley, A., Collins, W., Fillmore, D., Zender, C., and Coleman, D.: Impact of desert dust radiative forcing on Sahel precipitation: relative importance of dust compared to sea surface temperature variations, vegetation changes and greenhouse gaz warming, J. Climate, 20, 1445–1467, 2007.
Zakey, A. S., Solmon, F., and Giorgi, F.: Implementation and testing of a desert dust module in a regional climate model, Atmos. Chem. Phys., 6, 4687–4704, 2006, http://www.atmos-chem-phys.net/6/4687/2006/.

ACPD
10, 3053–3086, 2010

Table 1. Aerosol optical depth derived from RegCM for Dakar, Sal and Nouadhibou stations at 00:00 UTC and 12:00 UTC.

UTC	Dakar	Sal	Nouadhibou
00:00	0.38	0.51	1.86
12:00	0.17	0.70	1.34

ACPD

10, 3053–3086, 2010

Impacts of dust on West African climate during 2005 and 2006

M. Camara et al.

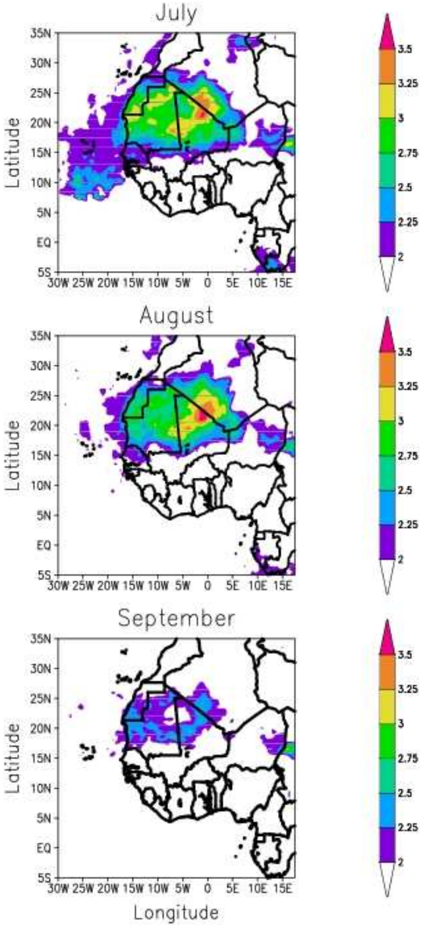

Fig. 1. Aerosol optical depth during July, August and September (left) and vertical profile of aerosol extinction coefficient (right) averaged over 10° W–0° W for July–August and over 10° W for September.

ACPD
10, 3053–3086, 2010

Impacts of dust on West African climate during 2005 and 2006

M. Camara et al.

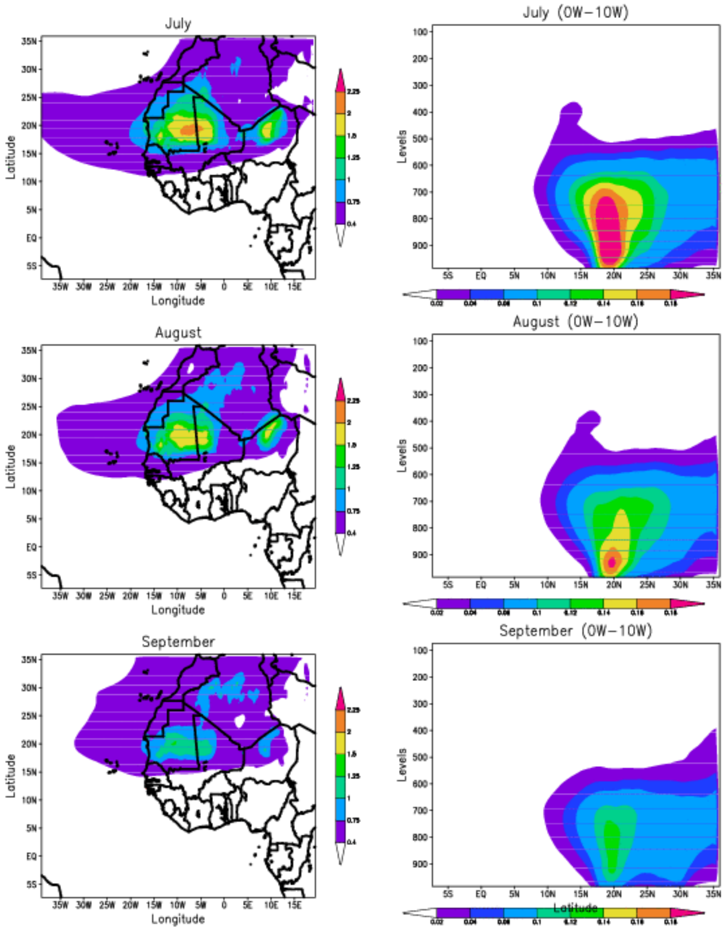

Fig. 2. TOMS aerosol index averaged over 2005–2006 for July, August and September period.

ACPD
10, 3053–3086, 2010

Impacts of dust on West African climate during 2005 and 2006

M. Camara et al.

Title Page
Abstract | Introduction
Conclusions | References
Tables | Figures
◂◂ | ▸▸
◂ | ▸
Back | Close
Full Screen / Esc
Printer-friendly Version
Interactive Discussion

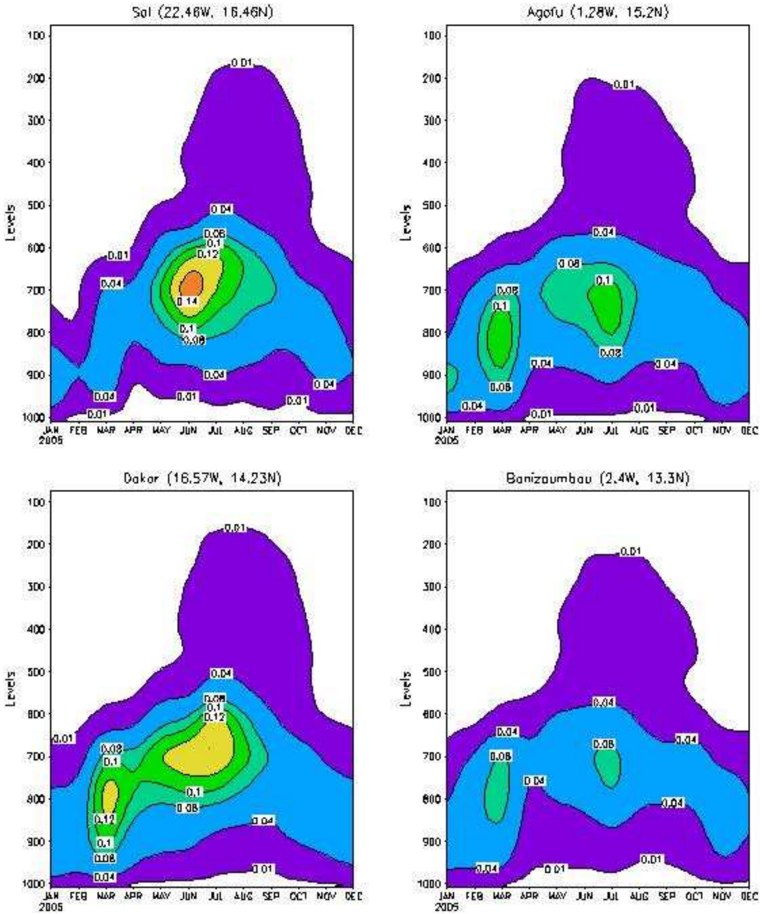

Fig. 3. Seasonal cycle of the profile of the aerosol extinction coefficient for the station of Dakar, Sal, Agoufu and Banizoumbou.

ACPD
10, 3053–3086, 2010

Impacts of dust on West African climate during 2005 and 2006

M. Camara et al.

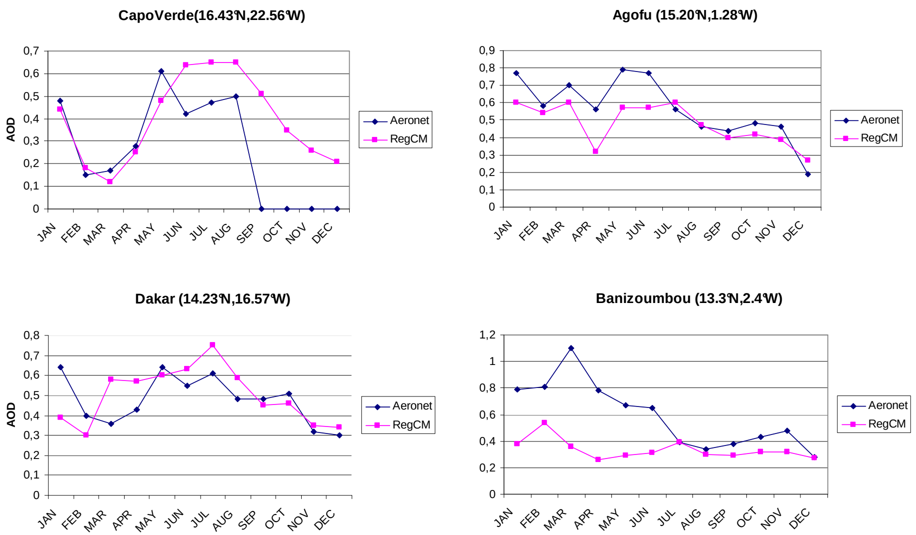

Fig. 4. Seasonal cycle of aerosol optical depth derived from RegCM and AERONET measurements during 2006 at Dakar, Sal, Agoufu and Banizoumbou.

ACPD

10, 3053–3086, 2010

ACPD

10, 3053–3086, 2010

Impacts of dust on West African climate during 2005 and 2006

M. Camara et al.

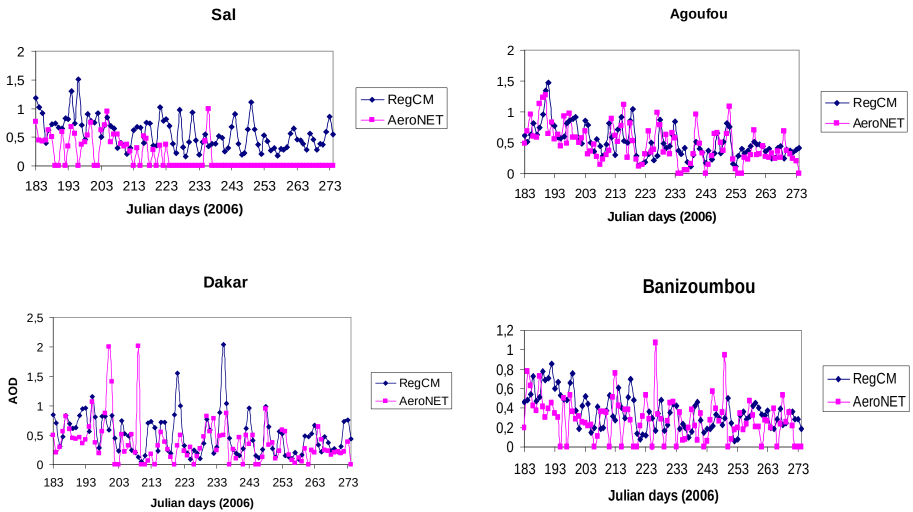

Fig. 5. Daily values of aerosol optical depth derived from RegCM and AERONET measurements during July–September 2006 at Dakar, Sal, Agoufu and Banizoumbou.

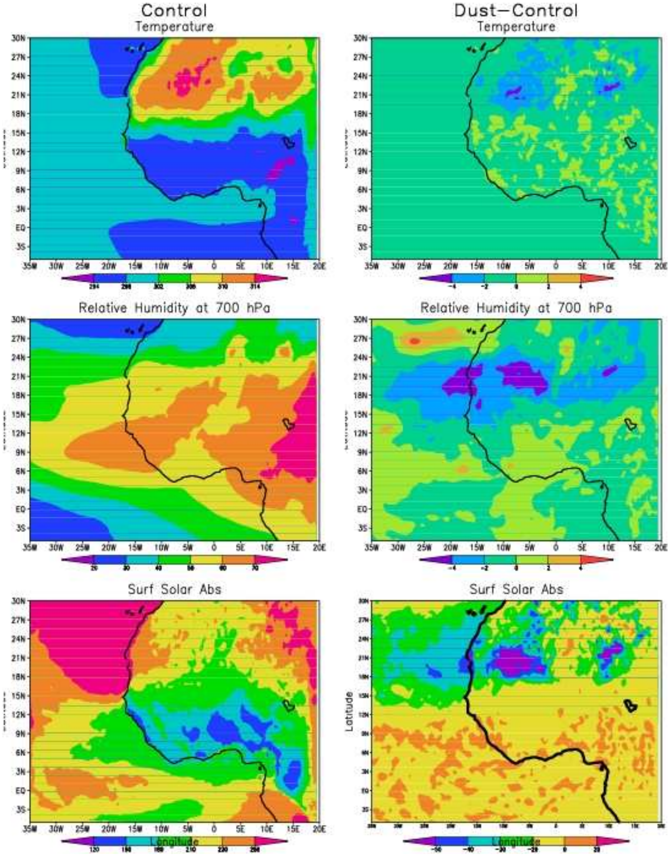

Fig. 6. Surface temperature (top), relative humidity (middle) and solar radiation absorbed at the surface (bottom) averaged during the July–September 2005–2006 period for the control case (left) and difference between dust and control case of surface temperature and specific humidity (right). Unit is ˚C for the temperature, % for the specific humidity and W for surface solar absorption.

ACPD
10, 3053–3086, 2010

Impacts of dust on West African climate during 2005 and 2006

M. Camara et al.

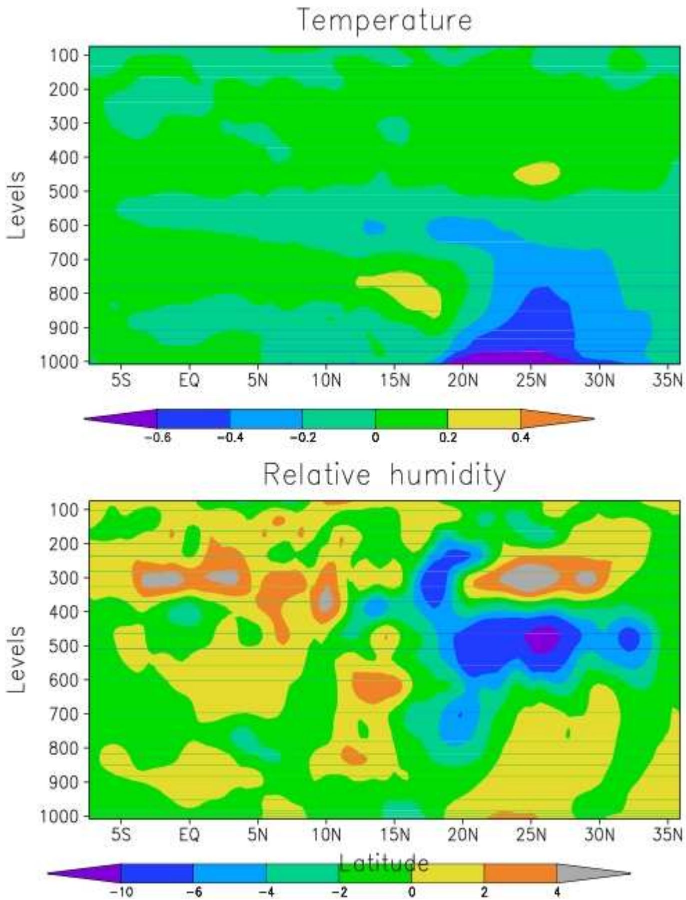

Fig. 7. Vertical profile of the difference between dust and control case of the temperature (top) and specific humidity (bottom) averaged during July–September 2005–2006. Unit is °C for the temperature and % for the relative humidity.

ACPD
10, 3053–3086, 2010

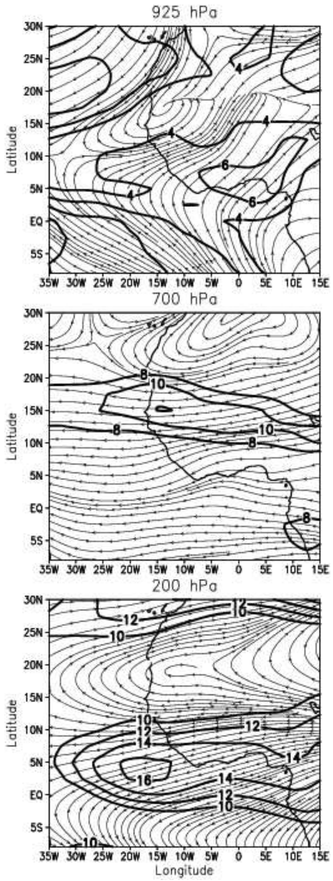

Fig. 8. Wind streamlines and module (contour) at 925 hPa, 700 hPa and 200 hPa for control (left) and the difference between dust and control cases (right) averaged during July–September 2005–2006. Unit is m/s for the module.

ACPD
10, 3053–3086, 2010

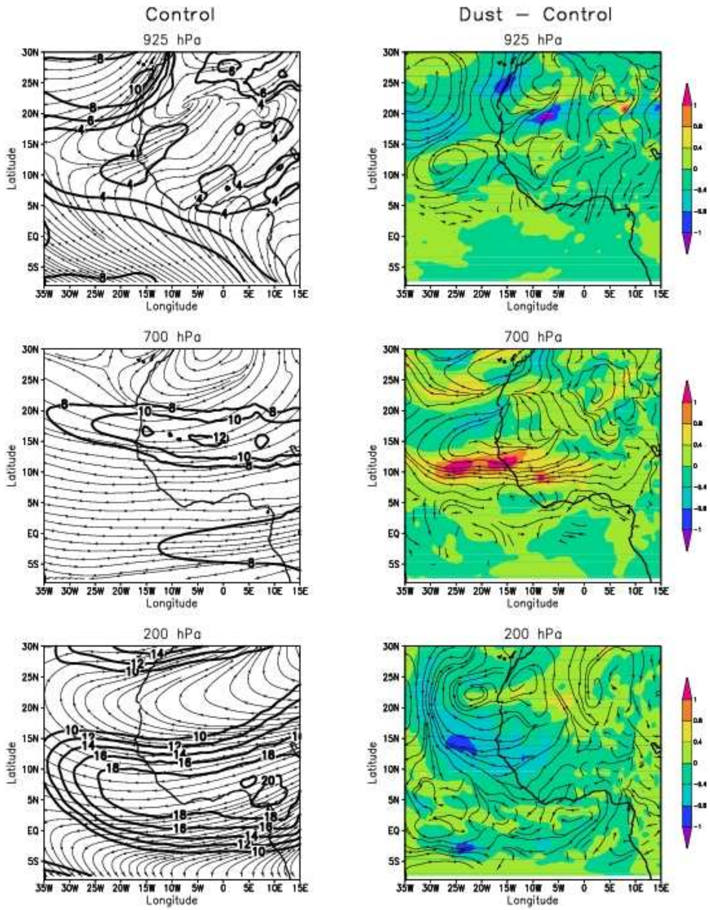

Fig. 9. NCEP/NCAR reanalysis wind streamlines and magnitude (contour) at 925 hPa, 700 hPa and 200 hPa averaged over July–September 2005–2006. Unit is m/s for the wind module.

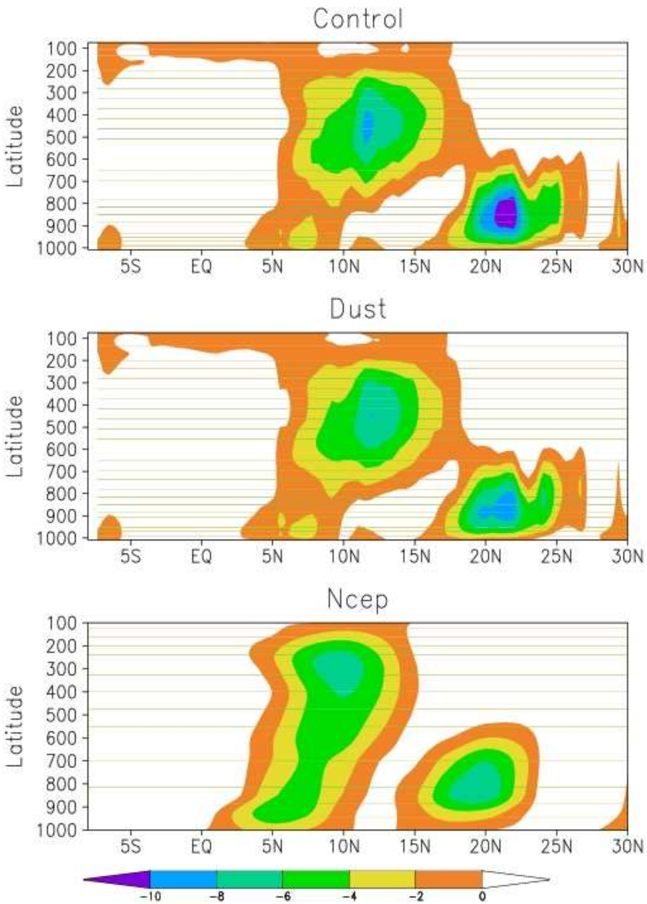

Fig. 10. Profile of Vertical velocity averaged between 10° W and 10° E for the control case (top), dust case (middle) and the NCE/NCAR reanalysis (bottom). Unit is 0.01 Pa/s.

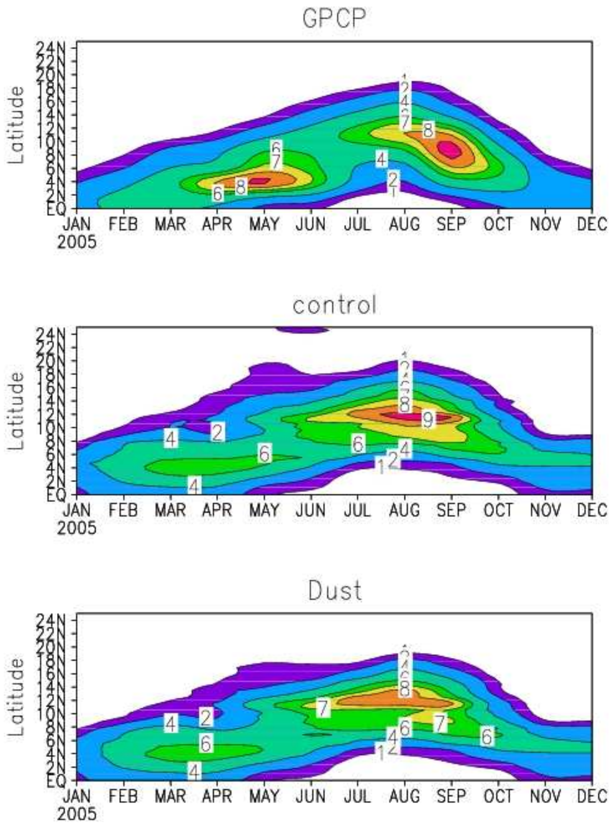

Fig. 11. Seasonal cycle of rainfall averaged between 10° W and 10° E for the GPCP data (top) control case (middle) and the dust case (bottom) during the mean 2005–2006. Unit is mm/day.

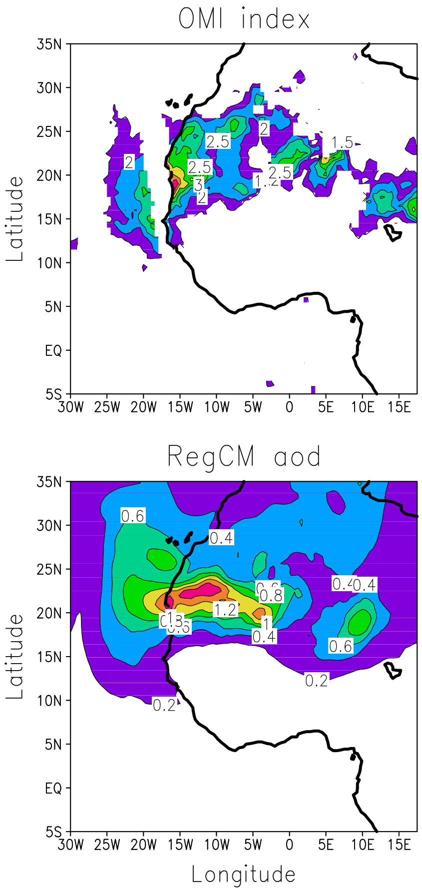

Fig. 12. TOMS aerosol index (top) and aerosol optical depth derived from RegCM (bottom) on 10 September 2006.

ACPD
10, 3053–3086, 2010

Impacts of dust on West African climate during 2005 and 2006

M. Camara et al.

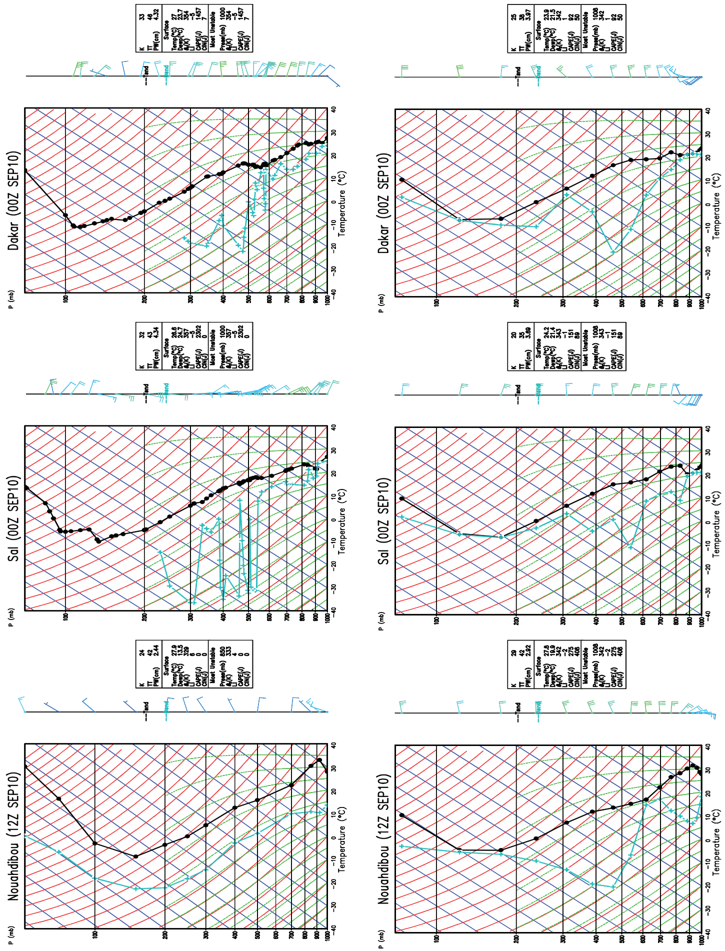

Fig. 13. Skew-T plot for the dust model (right) and the radiosounding data (left) at Dakar, Sal and Nouadhibou on 10 September 2006.

ACPD

10, 3053–3086, 2010

Impacts of dust on West African climate during 2005 and 2006

M. Camara et al.